STRUCTURAL AND MAGNETIC PROPERTIES OF HEUSLER ALLOYS Pd_2MnZ (Z=Ga, Ge, As): *AB INITIO* STUDY

Olga Miroshkina[1,*], *Mikhail* Zagrebin[1,2], *Vladimir* Sokolovskiy[1,3], and *Vasiliy* Buchelnikov[1]

[1]Chelyabinsk State University, 454001 Chelyabinsk, Russia
[2]National Research South Ural State University, 454080 Chelyabinsk, Russia
[3]National University of Science and Technology "MIS&S", 119991 Moscow, Russia

Abstract. In this work, we report results of *ab initio* and Monte Carlo investigations of structural and magnetic properties in a series of Heusler compositions Pd_2MnZ (Z = Ga, Ge, As). It was found that for Pd_2MnGa and Pd_2MnAs, the stable martensitic state is realized on the contrast with Pd_2MnGe. The equilibrium lattice parameters for the series of Pd_2MnZ (Z = Ga, Ge, As) compounds increase with increasing the number of valence electrons per atom (*e/a* ratio). Having calculated total magnetic moments and magnetic exchange parameters from *ab initio* methods, the Curie temperature for Pd_2Mn-based alloys has been estimated in the framework of Monte Carlo simulations of Heisenberg model.

1 Introduction

Heusler alloys are of great interest to the scientific community due to their unique properties such as shape memory effect, effects of superelasticity and superplasticity, giant magnetocaloric effect, giant magnetoresistance and magnetostrain, etc. These effects are associated with martensitic transformations [1-4].

Full-Heusler alloys are ternary intermetallic systems with $L2_1$ crystal structure and are derived from a parent compound with the generic formula X_2YZ. Here, X and Y are 3*d* transition metals, and Z are *sp* elements of III–V group of periodic table of elements.

At present, a small number of works is devoted to the study of Pd_2Mn-based alloys. For instance, Natera et al. found that Pd_2MnGe shows a preferentially disordered $L2_1$ structure with 0.98 Pd + 0.02 Mn on the A- and C-sites and 0.96 Mn + 0.04 Pd on the B-sites [5]. Yin and Nash measured enthalpies of formation of Pd_2MnGa (-54.5 ± 1.7 kJ/mol) [6].

The objective of this paper is the theoretical investigation of the structural and magnetic properties of Pd_2MnZ (*Z* = Ga, Ge, As) Heusler alloys and comparison with available experimental data.

2 Computational details

In this study, we used density functional formalism (DFT) as implemented in the Vienna ab-initio simulation program (VASP) [7, 8] and spin-polarized relativistic Korringa-Kohn-Rostoker (SPR-KKR) package [9] jointly with the classical Monte Carlo (MC) simulations. The generalized gradient approximation (GGA) in Perdew-Burke-Ernzerhoff parameterization [10] was considered in both VASP and SPR-KKR calculations.

In the first step, the structural ground state calculations were performed using the VASP package. In order to determine the presence of a stable martensitic state, calculations of the total energy as a function of the tetragonal distortion (c/a, where *a* and *c* are the crystallographic axis) of a cubic crystal are performed. Subsequently, the optimized structural configurations from the VASP calculations were used for the calculations of magnetic exchange constants by means of the SPR-KKR package.

Computational parameters used for the VASP package are following. The pseudopotentials were taken with the electronic configurations as follows: Pd ($4p^6 4d^9 5s^1$), Mn ($3p^6 3d^6 4s^1$), Ga ($3d^1 4s^2 4p^1$), Ge ($3d^1 4s^2 4p^2$), and As ($4s^2 4p^3$). The interaction between ions and electrons was described by the projector augmented wave (PAW) method [7, 8]. For the kinetic energy cut-off was 400 eV and the kinetic energy cut-off for the augmentation charges was 800 eV. Brillouin zone sampling was performed according to the Monkhorst-Pack grid [10]. The *k*-points for self-consistent field cycles in the Brillouin zone were generated with 12^3 meshes. All considered structures were relaxed using the conjugate gradient algorithm and both the atomic position and the volume were optimized.

As for the SPR-KKR package, the calculations of exchange parameters were performed using of the spin-polarized scalar-relativistic mode.

The Heusler compounds Pd_2MnZ (*Z* = Ga, Ge, As) possess the $L2_1$ type cubic structure with space group *Fm-3m* (No. 225). For present calculations, the conventional cell consisting of 4 atoms with a cell

* Corresponding author: miroshkina.on@yandex.ru

formula of Pd_2MnZ is used. The Ga, Ge, and As atoms locate on the 4*a* Wyckoff position with coordinate (0, 0, 0), the Pd atoms occupy 8*c* Wyckoff position with (1/4, 1/4, 1/4), and Mn atom possess 4*b* Wyckoff position with coordinate (1/2, 1/2, 1/2).

To obtain the temperature dependences of the magnetization of the Pd_2MnZ (Z = Ga, Ge, As) compounds, well-working and well-tested Heisenberg model was applied [11, 12, 13, 14]. With the use of long-range exchange interactions, it allows obtaining Curie temperatures close to the experiment. We carried out MC simulations of the three-dimensional Heisenberg model in the absence of anisotropy and magnetic fields

$$H_{mag} = -\sum_{\langle ij \rangle} J_{ij} \mathbf{S}_i \mathbf{S}_j \qquad (1)$$

where $\mathbf{S}_i$ is the spin of the unit length ($|\mathbf{S}_i| = 1$) placed at the lattice site, and J_{ij} are the exchange coupling parameters calculated using an expression proposed by Liechtenstein *et al.* [15]. The magnetic exchange parameters clearly show the damping oscillatory behavior, changing the type of interaction from ferromagnetic (FM) to antiferromagnetic (AFM) and vice versa. We included the exchange interactions up to eight coordination shell for all interaction pairs. The MC simulations were performed for a simulation cell with periodic boundary conditions using the Metropolis algorithm [16]. Therefore, for the Pd_2MnZ (Z = Ga, Ge, As) alloys, we used the simulation cell containing 1098 Pd, 1099 Mn, and 1728 Z atoms. Changes in the independent spin variables $\{S_i^x, S_i^y, S_i^z\}$ are accepted or rejected in accordance with the single-site transition probability, $W = min\{1; exp(-\Delta H/k_B T)\}$. As a time unit, we used one MC step consisting of N attempts to change the spin variables. For each temperature, the properties (internal energy of the system H and magnetic order parameter m) were analyzed, allowing 5×10^5 MC steps and 10^4 thermalization steps.

To calculate the total average magnetization M at a certain temperature point, we used the following equation:

$$M = 2\mu_{Pd} m_{Pd} + \mu_{Mn} m_{Mn}, \qquad (2)$$

where μ_{Pd} and μ_{Mn} are the magnetic moments of Pd and Mn atoms, which were obtained from *ab initio* calculations; m_{Pd} and m_{Mn} are the normalized magnetizations calculated as follows:

$$m_X = \frac{1}{N} \sum_i \sqrt{\left(S_i^x\right)^2 + \left(S_i^y\right)^2 + \left(S_i^z\right)^2}. \qquad (3)$$

3 Results and discussion

3.1 Structural properties

Initially, we determined the equilibrium lattice constant of a crystal of Pd_2MnZ compounds using the geometry optimization in VASP, focusing on the equilibrium volume of the cell and the tetragonal distortion parameterized by the *c/a* ratio. In this case, a negligibly small change in volume between the cubic and tetragonal phases was assumed: $V_0 = a_0^3 = a^2 c$.

The calculated equilibrium lattice parameters and bulk modulus of the Pd_2MnZ austenitic compounds are summarized in Table 1. Noted parameters were estimated according to the Birch-Murnagahan equation of state. As one can see from Table 1, the equilibrium lattice parameters for a series of Pd_2MnZ (Z = Ga, Ge, As) compounds increase with increasing *e/a* due to increasing Z element's radius. Experimental values of Pd_2MnGa and Pd_2MnGe are 6.180 Å and 6.174 Å, respectively [17].

Table 1. Calculated lattice constants a_0 (in Å) and bulk modulus B (in GPa) for Pd_2MnZ alloys

Compound	*e/a*	a_0	B
Pd_2MnGa	7.50	6.212	142.7
Pd_2MnGe	7.75	6.237	127.8
Pd_2MnAs	8.00	6.301	129.2

In order to investigate the possibility of the martensitic transformation in alloys studied, we performed calculations of the total energy relative to the cubic phase as a function of the tetragonality ratio *c/a*. The total energy differences between the tetragonally distorted and the cubic phases as functions of *c/a* ratio for Pd_2MnZ (Z = Ga, Ge, As) alloys are shown in Fig. 1. In this case, ΔE = 0 corresponds to the equilibrium austenitic phase for each compound.

It is seen that for Pd_2MnGa and Pd_2MnAs, the stable martensite can be realized at *c/a* ratio of 1.30 and 1.35, respectively. While in the case of the stoichiometric Pd_2MnGe alloy, the austenite–martensite transformation does not occur due to the absence of any energy minima in the $E(c/a)$ curve for $c/a \neq 1$, as shown in Fig. 1.

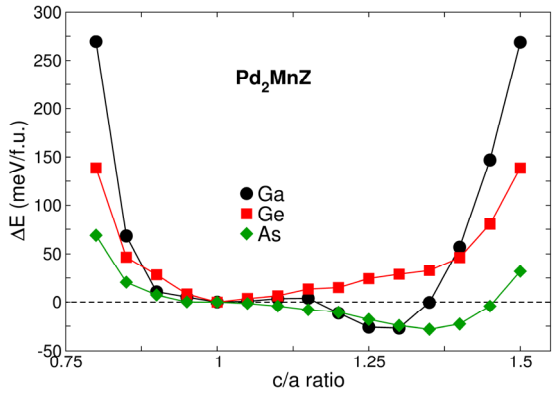

Fig. 1. The total energy differences with respect to equilibrium value for a series of Pd_2MnZ (Z = Ga, Ge, As) alloys as functions of tetragonal distortion, *c/a*.

3.2 Electronic and magnetic properties

The total densities of the electronic states are shown in Fig. 2(a-c). The analysis of the densities of electron states shows the relative shift of the Fermi level to higher energy regions in the Ga-Ge-As sequence, which arises

from the increase in the number of valence electrons in this series of alloys. The character of the densities of electronic states is similar to those obtained for other Pd_2Mn-containing alloys [18, 19].

Magnetic properties of Pd_2Mn-based series of alloys are also of significant interest, because they allow us to predict compositional trends of the Curie temperature.

Firstly, the total magnetic moment of Pd_2MnZ (Z = Ga, Ge, As) compounds was calculated using the SPR-KKR package. We found that Pd_2MnGa possesses the lowest magnetic moment (4.12 μB/f.u.) and it increases slightly with the increasing number of valence electrons per atom e/a. Whereat we evaluated the magnetic exchange parameters.

The exchange coupling constants, J_{ij}, for Pd_2MnZ as a function of the distance between interacting atoms i and j are shown in Fig. 2 (d-f).

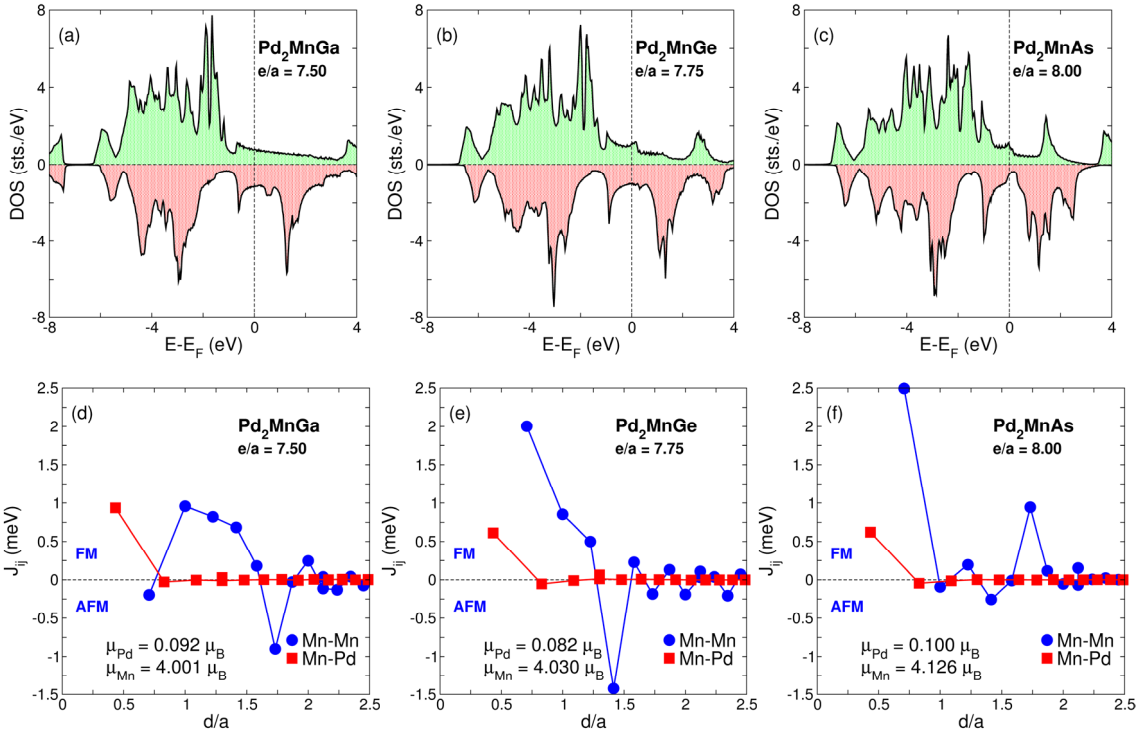

Fig. 2. The total densities of the electronic states and the exchange coupling parameters for (a) Pd_2MnGa, (b) Pd_2MnGe, and (c) Pd_2MnAs alloys as a function of the distance (d/a) between atoms i and j. Here a is the optimized lattice parameter.

It is worth mentioning that positive values of J_{ij} correspond to the FM exchange, whereas the negative ones mark the AFM exchange. It should be noticed that exchange interactions between Pd-Z (Z = Ga, Ge, As) and Pd-Pd atoms are very small due to the lowest magnetic moments and omitted from the figures. It is seen that for all compounds studied the Mn-Pd pair exhibits a similar behavior, where the nearest-neighbor interactions provide the maximum contribution to the exchange energy than subsequent interactions. The latter ones are close to zero.

As for the Mn-Mn exchange interactions, they have an AFM character between nearest-neighbor atoms within the first coordination shell for Pd_2MnGa, then it becomes FM and increases slightly with increasing e/a ratio. The magnetic exchange parameters clearly show the damping oscillatory behavior for all compositions, which can be associated with various exchange mechanisms such as the magnetic interaction between localized d and collectivized s electrons, magnetic exchange interaction between localized and collectivized d electrons, and super-exchange interaction via sp-conduction electrons contributing to the RKKY-type indirect exchange interaction [18]. In addition, for Pd_2MnGa and Pd_2MnGe, the AFM contributions to the exchange energy are accounted for Mn-Mn interactions within the sixth and fourth coordination shells, respectively. On the other side, for Pd_2MnAs, the AFM contributions are significantly less than for other alloys of studying series.

Obtained exchange coupling parameters and partial magnetic moments for Pd_2MnZ (Z = Ga, Ge, As) alloys were used for further MC simulations of the thermomagnetization curves to obtain corresponding Curie temperatures. The set of magnetization curves as a function of temperature for alloys studied is presented in Fig. 3. As can be seen from Fig. 3, for all cases, the ferromagnetic – paramagnetic phase transition in austenite occurs. In a case of Pd_2MnGa, the highest Curie temperature can be observed due to Mn-Mn FM interactions within second, third, fourth, and fifth coordination shells jointly with nearest-neighbor Mn-Pd FM interaction. On the other hand, for Pd_2MnGe, the lowest value of Curie temperature is found because of the largest AFM contribution between Mn atoms interacting within the fourth shell. We note that the experimental value of Curie temperature of Pd_2MnGe is 170 K [17].

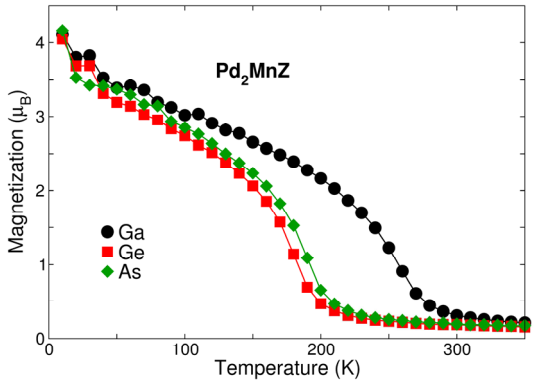

Fig. 3. Magnetization curves of Pd_2MnZ (Z = Ga, Ge, As) as a function of temperature.

The calculated total magnetic moments and Curie temperatures for alloys studied are summarized in Table 2.

Table 2. Calculated total magnetic moment μ_{tot} (in μ_B/f.u.) and Curie temperature T_C (in K) for Pd_2MnZ (Z=Ga, Ge, As) alloys

Compound	*e/a*	μ_{tot}	T_C
Pd_2MnGa	7.50	4.12	255
Pd_2MnGe	7.75	4.14	183
Pd_2MnAs	8.00	4.27	198

4 Conclusion

The optimized lattice parameters for austenite and martensite, total magnetic moments as well as thermomagnetization curves and Curie temperatures for a series of Pd_2MnZ (Z = Ga, Ge, As) compounds are successfully obtained using the first-principles ground state calculations in association with the finite-temperature Monte Carlo simulations. *Ab initio* calculations were performed using VASP and SPR-KKR packages.

It was shown that the optimized lattice parameters of considered alloys increase along the sequence of $Pd_2MnGa \rightarrow Pd_2MnGe \rightarrow Pd_2MnAs$. This has to do with the fact that Z element's radius increases along the respective sequence. The lattice energy calculations for the distorted cubic structure have shown that the stable martensitic phase can be realized only for Pd_2MnGa and Pd_2MnAs compounds with *c/a* ratio of 1.3 and 1.35, respectively. The total magnetic moments for the cubic austenitic state of Pd_2MnZ (Z = Ga, Ge, As) were found to be increasing with the increasing *e/a* ratio. Using the Heisenberg Hamiltonian and exchange coupling constants, the Curie temperatures for compounds studied have been obtained. It was shown that Pd_2MnGa possesses the Curie temperature close to room temperature, while for remaining compositions, it found to be around 190 K. We consider that discussed alloys could be interesting for further investigations.

Acknowledgments

This work was supported by Russian Science Foundation No. 17-72-20022\17 (VASP calculations) and Russian Science Foundation No. 14-22-00279 (SPR-KKR calculations).

References

1. P. Entel, V.D. Buchelnikov, V.V. Khovailo et al, J. Phys. D: Appl. Phys., **39**, 865 (2006)
2. V.D. Buchelnikov, A.N. Vasiliev, V.V. Koledov et al, Phys.-Usp., **49**, 871 (2006)
3. P. Entel, M. E. Gruner, A. Dannenberg, Mat. Sci. Forum, **635**, 3 (2010)
4. P.J. Webster, K.R.A. Ziebeck, S.L. Town, M.S. Peak, Philos. Mag. B, **49**, 295 (1984)
5. M.G. Natera, M.R.L.N. Murthy, R.J. Begum, and N.S. Satya Murthy, Phys. Status Solidi A, **3**, 959 (1970)
6. M. Yin, P. Nash, Intermetallics, **58**, 15 (2015)
7. G. Kresse, J. Furthmuller, Phys. Rev. B, **54**, 11169 (1996)
8. G. Kresse, D. Joubert, Phys. Rev. B, **59**, 1758 (1999)
9. H. Ebert, D. Kodderitzsch, J. Minar, Rep. Prog. Phys., **74**, 096501 (2011)
10. J.P. Perdew, K. Burke, M. Enzerhof, Phys. Rev. Lett., **77**, 3865 (1996)
11. P. Yu, X.F. Jin, J. Kudrnovský, D.S. Wang et al, Phys. Rev. B, **77**, 054431 (2008)
12. D. Comtesse, H.C. Herper, A. Hucht and P. Entel, Eur. Phys. J. B, **85**, 10 (2012)
13. D. Böttcher, A. Ernst, J. Henk, J. Magn. Magn. Mater., **324**, 610 (2012)
14. V.V. Sokolovskiy, V.D. Buchelnikov, M.A. Zagrebin et al, Phys. Rev. B, **86**, 134418 (2012)
15. A. Liechtenstein, M. Katsnelson, V. Antropov et al, J. Magn. Magn. Mater., **67**, 65 (1987)
16. D.P. Landau, K. Binder, *A Guide to Monte Carlo Simulations in Statistical Physics* (Cambridge University Press, Cambridge, 2005)
17. P.J. Webster *The Magnetic and Chemical Structures of the Heusler Alloys* (University of Sheffield, Sheffield, 1968)
18. E. Şaşıoğlu, L.M. Sandratskii, P. Bruno, Phys. Rev. B, **77**, 064417 (2008)
19. J. Kübler, A.R. William, C.B. Sommers, Phys. Rev. B, **28**, 1745 (1983)